ARTICLE

Photopatternable Poly(4-styrene sulfonic acid)-Wrapped MWNT Thin-Film Source/Drain Electrodes for Use in Organic Field-Effect Transistors

Kipyo Hong,[†] Se Hyun Kim,[†] Chanwoo Yang,[†] Won Min Yun,[†] Sooji Nam,[†] Jaeyoung Jang,[†] Chanjun Park,[‡] and Chan Eon Park*[,†]

Polymer Research Institute, Department of Chemical Engineering, Pohang University of Science and Technology, Pohang, 790-784, Korea, and Department of Mechanical Engineering, Seoul National University of Science and Technology, Seoul, 139-743, Korea

ABSTRACT We describe the cross-linking of poly(4-styrene-sulfonic acid) (PSS) by exposure to ultraviolet (UV) light ($\lambda = 255$ nm) under a vacuum. Fourier transform infrared (FT-IR) spectroscopy and X-ray photoelectron spectroscopy (XPS) showed that the photo-crosslinking of PSS resulted from coupling between radicals that were generated in the polymer chains by UV excitation. The photo-cross-linkable characteristics of PSS were employed to fabricate solution-processable, photopatternable, and conductive PSS-wrapped multiwalled carbon nanotube (MWNT) composite thin films by wrapping MWNTs with PSS in water. During photo-cross-linking, the work function of the PSS-wrapped MWNTs decreased from 4.83 to 4.53 eV following cleavage of a significant number of sulfonic acid groups. Despite the decreased work function of the PSS-wrapped MWNTs, the photopatterned PSS-wrapped MWNTs produced good source/drain electrodes for OFETs, yielding a mobility (0.134 ± 0.056 cm^2/(V s)) for the TIPS-PEN field-effect transistors fabricated using PSS-wrapped MWNTs as source/drain electrodes that was higher than the mobility of gold-based transistors (0.011 ± 0.004 cm^2/(V s)).

KEYWORDS: solution-processable • photopatternable • source/drain electrodes • carbon nanotube • organic field-effect transistor • contact resistance

INTRODUCTION

Organic field-effect transistors (OFET) have received considerable attention because of their potential uses in cheap, light, flexible, transparent, and disposable electronic products, such as portable displays, smart cards, and radio frequency identification tags (1−3). To realize these applications, organic materials that are solution-processable at low temperatures must be developed to replace current high-cost vacuum-deposited organic materials, such as pentacene and C_{60}. Recent developments in solution-processable organic semiconductors composed of small molecules and polymers, such as 6,13-bis(triisopropylsilylethynyl) pentacene (TIPS-PEN), poly(3-hexylthiophene), and poly(2,5-bis(3-alkylthiophen-2-yl)thieno[3,2-b]thiophene), have made it possible to achieve device performances comparable to those of amorphous silicon transistors (4−6).

Source/drain electrodes in OFETs should have high work functions (for p-type transistors) and high conductivities. To date, many materials, including conductive polymers, silver paste, and graphene, have been tested as possible electrodes for OFETs. Carbon nanotubes are also good candidate materials for electrodes in flexible organic devices because of their high conductivity and mechanical strength (7, 8); however, poor solubility has limited their use. Carbon nanotubes can be solubilized in water by the addition of small-molecule surfactants (9, 10) or conductive polymers (11), or by wrapping the nanotubes with polyelectrolytes such as poly(acrylic acid), poly(4-styrene sulfonic acid) (PSS), or poly(allylamine) (12−15). Fabricated carbon nanotube thin films have been characterized by flexibility, high transparency, and high conductivities up to 1×10^3 S/cm. They have been applied as electrodes in various organic electronic devices, such as OFETs (15−17), organic light-emitting diodes (18, 19), and organic solar cells (10, 20), and showed good device performance.

The patterning of source/drain solution-processable electrode materials is a key issue for OFET fabrication. To date, a variety of techniques have been developed to pattern source/drain electrodes, including inkjet printing, contact printing, imprinting, screen printing, spray printing, and selective-organization techniques (21−27). The low costs associated with solution processing of electrode materials are desirable for realizing low-cost organic devices. Currently, printing methods are more advantageous than conventional photolithographic procedures, which usually involve several steps, including the use of a photoresist, which

* Corresponding author. E-mail:cep@postech.ac.kr. Tel: +82-54-279-2269. Fax: +82-54-279-8298.
Received for review September 15, 2010 and accepted December 1, 2010
[†] Pohang University of Science and Technology.
[‡] Seoul National University of Science and Technology.
DOI: 10.1021/am1008826

Published on Web 12/13/2010

leads to a high process cost. If the source/drain electrode materials are photo-cross-linkable, photolithography can be employed for the production of organic thin film transistors at low cost by removing the need for a photoresist, thereby decreasing the number of fabrication steps. Because photo-cross-linked materials are insoluble in most common solvents, they permit deposition of solution-processable organic semiconductors in organic solvents on electrode-patterned substrates. Very few materials, for example, poly(3,4-ethylenedioxythiophene):poly(styrene sulfonate) (PEDOT:PSS) with bis(fluorinated phenyl azide) (or 4,4′-diazido-2,2′-disulfonic acid benzalacetone disodium salt) and silver pastes composed of photoactive polymers, have been tested for use as photopatternable electrodes (28−31). In the present work, we found out PSS without a photo-crosslinker could be photo-crosslinked by exposure to ultraviolet (UV) light (255 nm) under a vacuum. The fabricated PSS-wrapped MWNTs were also photo-cross-linkable because the MWNT surfaces were coated with the photo-cross-linkable PSS. We fabricated TIPS-PEN transistors using PSS-wrapped MWNT source/drain electrodes by photopatterning and showed that the photopatterned PSS-wrapped MWNTs produced good source/drain electrodes in OFETs.

EXPERIMENTAL SECTION

Materials and Sample Preparation. The MWNTs and PSS ($M_w \approx 75\,000$) were purchased from Carbon Nanomaterial Technology Co. Ltd, Korea and Aldrich, respectively. The MWNTs were used as received. The nanotubes were dispersed in a 1.5 wt % solution of PSS in water (at a concentration of 15 mg/mL) by ultrasonication for 30 min. The PSS/MWNT solution was then centrifuged at a rotor speed of 7500 rpm for 20 min, which corresponded to 8700 *g*. The resulting homogeneous dispersion of as-prepared PSS-wrapped MWNTs was stable, and no phase separation or aggregation of nanotubes was observed, not even after 2 weeks. Photo-cross-linking of PSS-wrapped MWNTs was carried out in a small vacuum chamber ($\sim 1 \times 10^{-3}$ Torr) equipped with a quartz window. The PSS-wrapped MWNT film was exposed to UV light ($\lambda = 255$ nm, power = 50 W) (G15T8, Sankyo Denki) through the quartz window over a distance of 10 cm.

Characterization. The resistivity of a PSS-wrapped MWNT film spin-coated onto a glass substrate was calculated from the sheet resistance measured using the four-point probe method (Keithley 2400 Sourcemeter). The film thickness was measured using a surface profiler (Alpha-step 500, TENCOR). The PSS-wrapped MWNTs and photo-crosslinked MWNTs spin-coated onto the gold substrate were characterized by ultraviolet photoelectron spectroscopy (UPS) (Escalab 220IXL) using the He(I) emission line at 21.2 eV to measure the work function. During UPS measurements, a −5.0 eV bias was applied to improve the transmission of low kinetic energy electrons and determine the energy of the low kinetic energy edge.

Device Fabrication. OFETs with bottom-contact configurations, in which the source/drain electrodes were constructed prior to depositing the semiconductor layer, were fabricated on heavily doped silicon wafers covered by thermally grown 300 nm thick silicon dioxide layers. The substrates were modified with hexamethyldisilazane (HMDS) after rinsing with acetone and cleaning with a UV-ozone cleaner, GCS-1700 (Ahtech Lts, Korea), for 20 min. The PSS-wrapped MWNT solution was spin-coated onto these substrates, and the substrates were loaded into the vacuum chamber. The coated substrate was subsequently exposed to UV light through a shadow mask for 40 min

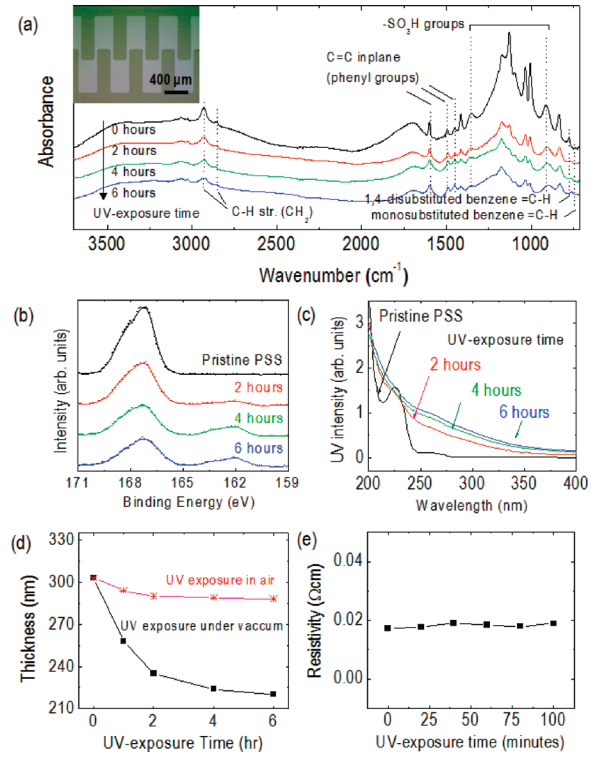

FIGURE 1. (a) FT-IR spectra of PSS films exposed to UV under a vacuum for 0, 2, 4, and 6 h. The inset shows the patterned PSS polymer geometry. (b) XPS spectra of S2p with Al Kα ($h\nu = 1486.6$ eV) for the as-loaded PSS and the UV-exposed PSS for 2, 4, and 6 h under a vacuum. (c) UV−visible absorption spectra of PSS films on quartz as a function of UV exposure time. (d) Thickness of PSS films exposed to UV in air or under a vacuum as a function of time. (e) Resistivity of PSS-wrapped MWNT films as a function of UV exposure time.

then developed in water to remove any un-cross-linked materials. The channel lengths (*L*) and widths (*W*) of the patterned 50 nm thick source/drain electrodes were 100 μm and 1000 μm, respectively. A solution of TIPS-PEN in toluene (1 wt %) was dropped onto the patterned substrates and dried under ambient conditions. The electrical characteristics of the OFETs were measured in air using Keithley 2400 and 236 source/measure units.

RESULTS AND DISCUSSION

Polystyrene and halogenated polystyrene are photo-crosslinkable by irradiation with 255 nm ultraviolet (UV) light, enabling photopatterning of these polymers (32). If irradiation is conducted in air, the radicals generated by UV irradiation react with oxygen, leading to oxidation and degradation of the polymer. However, if UV irradiation is conducted in an oxygen-free atmosphere, such as under a vacuum or in a nitrogen atmosphere, the radicals react with other radicals, resulting in cross-linking. This implies that the polystyrene-based polymer, PSS, is photo-cross-linkable.

The inset of Figure 1a shows an optical microscopy image of the photopatterned PSS obtained by exposure to UV for 2 h under a vacuum. Transmission Fourier transform infrared (FT-IR) spectra were collected from a 200 nm thick PSS film on silicon wafer at several time points during UV exposure, from 0 to 6 h (Figure 1a). Polystyrene radicals are normally generated by the cleavage of an α-hydrogen bond, which is sensitive to light and has a low bond-dissociation

Scheme 1. Possible Reactions of PSS, Including the Cross-linking Reaction, Generated by UV Light Exposure

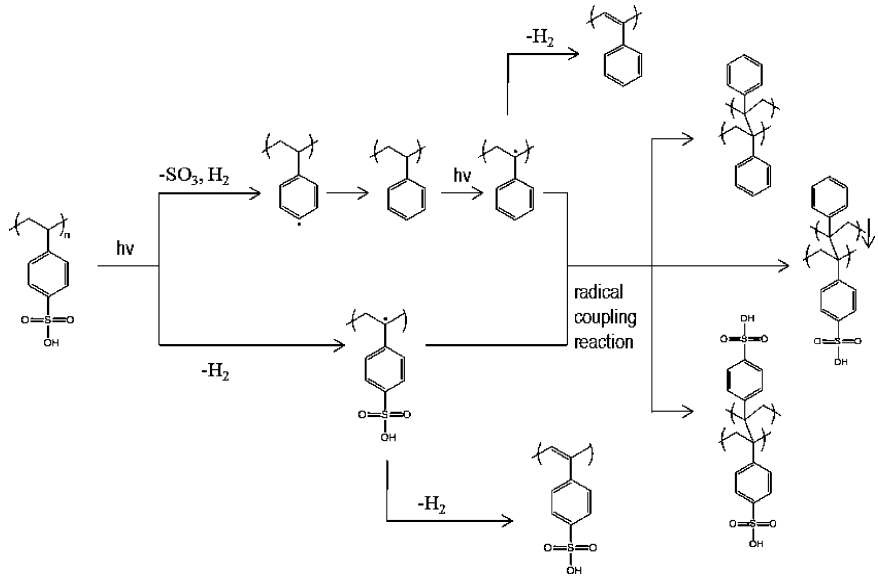

energy. The α-radicals react with other α-radicals, producing radical−radical coupling reactions (32). As the UV exposure time increased, we observed a reduction in the intensities of the peaks corresponding to the C−H symmetric and asymmetric stretching vibrations (2849 and 2931 cm^{-1}, respectively) of the $-CH_2-$ groups. This observation indicates that the UV-generated radicals formed via cleavage of α-hydrogen atoms on the chain, which then reacted with other radicals to cross-link the PSS chains.

A large shift in the $-SO_3H$ peak, from 912 to 1351 cm^{-1}, was observed as the UV exposure progressed. The reduction implied cleavage of the sulfonic acid groups from the phenyl group, similar to the cleavage observed for halogens from halogenated polystyrenes during exposure to 255 nm UV light (32). Cleavage of the sulfonic acid group was more clearly observed in the significant attenuation in peak intensity of the S2p orbital in the X-ray photoemission spectra (XPS) (Figure 1b) (33). However, the radical that formed via cleavage of the sulfonic acid group did not lead to cross-linking, as was evident from significant decrease in the C−H vibrational modes of the *p*-disubstituted phenyl group at 775, 835, and 1413 cm^{-1} and the increase in the C−H mode of the monosubstituted phenyl groups at 761 cm^{-1} (34). Because phenyl radicals that are formed by cleavage of sulfonic acid are generally short-lived and immediately form a benzene ring, they cannot be involved in a radical−radical coupling reaction (32).

Figure 1c shows the UV−visible absorption spectra of pristine PSS and a UV-exposed PSS films on quartz as a function of UV exposure time. As the UV exposure time increased from 0 to 6 h, the absorption at longer wavelengths increased due to double bond formation in the polymer chain. This implies that UV-generated radicals in the chain cannot only react with other radicals but they also converted to stable double bond formation via α-hydrogen abstraction (32, 35). The C═C mode of the double bonds produced was not clearly observed in the FT-IR spectra because the broad band from 1620 to 1680 cm^{-1} overlapped with both the broad band of the C═C bending vibration from the phenyl groups at 1600 cm^{-1} and the O−H bending vibration of the sulfonic acid group at 1680 cm^{-1}.

Scheme 1shows the possible reactions of PSS, including the crosslinking reaction produced by UV light exposure. After UV exposure, the PSS film became insoluble in water and organic solvents due to the cross-linking. During UV exposure under vacuum, the thickness of the PSS film decreased significantly, which is a general indicator of cross-linking (Figure 1d). It is because cross-linking decreases free volume between polymer chains. However, when the PSS film was exposed to UV radiation in air, the thickness did not change significantly, and the film became sticky because of cleavage, oxidation, and degradation of the PSS polymer chains.

Because the PSS polymer is photo-crosslinkable, PSS-wrapped MWNTs are photopatternable (Figure 2a). The PSS-wrapped MWNTs could be photopatterned with a spatial resolution of 10 μm. However, whereas PSS required UV exposure for more than 2 h for patterning, the UV exposure time required for photopatterning of the PSS-wrapped MWNTs was 40 min. The shortened time was probably due to the decreased presence of water-soluble PSS in the composite material. Although a 40 min exposure time is still relatively long, optimization of the UV power and distance between the UV lamp and the sample may reduce this exposure time. The measured resistivity of the PSS-wrapped MWNT films was 0.017 Ω cm (conductivity of about 60 S/cm). At UV exposure times between 20 and 100 min, the resistivity remained unchanged (Figure 1e), implying that UV exposure did not chemically alter the nanotubes. Images b and c in Figure 2 show SEM images of the pristine MWNT powder and the spin-coated PSS-wrapped MWNT film, respectively. The surface of the pristine MWNTs was smooth, whereas the surface of nanotubes in the PSS-wrapped MWNT film was rough, implying that the nanotubes were covered with PSS.

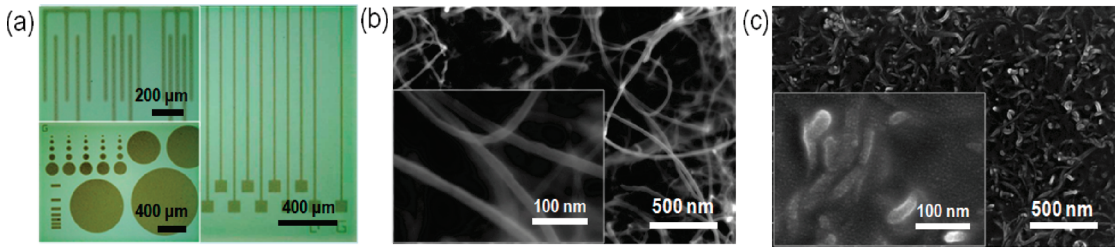

FIGURE 2. (a) Optical microscopy images of photo-patterned PSS-wrapped MWNT electrodes, (b) SEM images of the pristine MWNT powder, and (c) spin-coated film of cross-linked PSS-wrapped MWNTs.

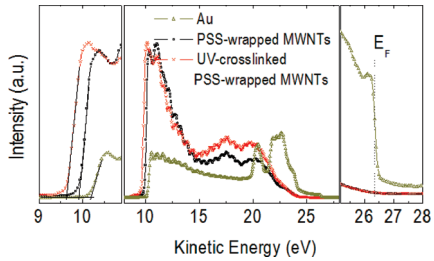

FIGURE 3. Middle: Full UPS spectra of PSS-wrapped MWNTs, UV-cross-linked PSS-wrapped MWNTs, and gold. Left: Close-up of the cut-off electron region used to determine the work function. Right: Close-up of the Fermi edge of the photoemission region.

The work functions of the PSS-wrapped MWNTs and UV-exposed PSS-wrapped MWNTs were measured by UPS (Figure 3). The low kinetic energy edge on the left-hand side of each UP spectrum (E_k^{min}) corresponds to electrons that have just sufficient energy to escape from the solid, and thus gives information about the position of the vacuum level. The maximum kinetic energy (E_k^{max}) on the right-hand side of each UP spectrum corresponds to electrons from the highest occupied level and therefore provides information about the position of the Fermi level (E_F). E_k^{max} and E_k^{min} were determined through linear extrapolation of the UP spectra. The work functions Φ_m were obtained by using the equation $\Phi_m = h\nu - (E_k^{max} - E_k^{min})$ (36). The work function of PSS-wrapped MWNTs was 4.83 eV. This work function was reduced to 4.53 eV after UV exposure. Previously, we reported that the work function of MWNTs (4.47 eV) increased after wrapping the MWNTs with PSS as a result of the negative dipole moment of the PSS's pendant groups, which were oriented away from the nanotube surface (15). Thus, when PSS-wrapped MWNTs were exposed to UV light, cleavage of the sulfonic acid groups lowered the work function. However, despite a reduced work function, the PSS-wrapped MWNTs were still appropriate for use as source/drain electrodes in OFETs. Typical drain current−gate voltage transfer curves for TIPS-PEN field-effect transistors, fabricated using PSS-wrapped MWNT source/drain electrodes photopatterned by exposure to UV, are shown in Figure 4b. The carrier mobility was calculated in the linear regime from the slope of the drain current as a function of gate voltage. Th calculation was performed by fitting the data to the following equation e: $I_D = (WC_i/L)\mu(V_G - V_{th})V_D$, where I_D is the drain current, μ is the carrier mobility, V_{th} is the threshold voltage, V_G is the gate voltage, and V_D is the drain voltage (namely, −4 V) (37). The measured capacitance, C_i, was 10 nF/cm^2. The average field-effect mobility of the pentacene OFETs composed of photopatterned PSS-wrapped

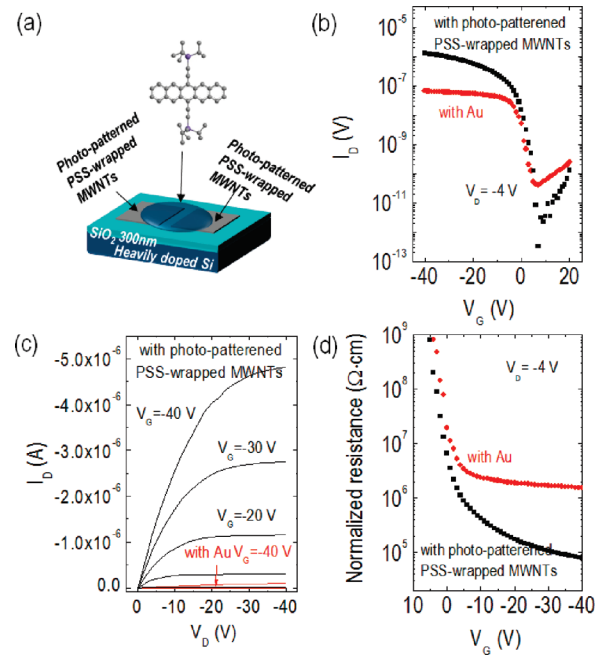

FIGURE 4. (a) Schematic diagram of a TIPS-PEN bottom-contact OFET containing PSS-wrapped MWNT electrodes, (b) transfer characteristics, (c) output characteristics of OFETs composed of UV-patterned PSS-wrapped MWNTs and Au electrodes, and (d) width-normalized total resistance, including channel and contact resistances in an OFET, as a function of gate voltage.

MWNT source/drain electrodes was 0.134 ± 0.056 cm^2/(V s) with an on/off ratio of 1.5 × 10^5. In contrast, the average field-effect mobility of the devices based on gold substrates was 0.011 ± 0.004 cm^2/V · s with an on/off ratio of 2.8 × 10^3, which is consistent with the previous reports (38, 39). The devices fabricated from the nanotubes showed ohmic contact behavior (Figure 4c), implying negligible contact resistance between photopatterned PSS-wrapped MWNTs and the TIPS-PEN transistors. Figure 4d shows the width-normalized total resistance, RW, of transistors fabricated with gold and photopatterned PSS-wrapped MWNT electrodes, which is the sum of the channel resistance and the contact resistance as a function of V_G, at a V_D of −4 V. RW is given by

$$RW = R_C W + \frac{L}{\mu C_i (V_G - V_{th})}$$

where $R_C W$ is the width-normalized contact resistance. During the sweep of V_G from 0 to −10 V, the RW of the device fabricated with gold decreased by reduction of the

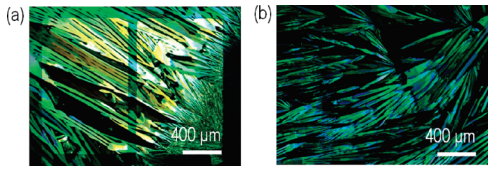

FIGURE 5. (a) Polarized optical microscopy of TIPS-PEN polycrystalline films on a gold-patterned substrate and (b) on a PSS-wrapped MWNT-patterned substrate.

channel resistance because the channel resistance is inversely proportional to V_G. From a V_G of −10 V, RW was almost unchanged despite increases in V_G. This is because R_CW was large and the changes in channel resistance as a function of V_G were negligible compared to R_CW, indicating that the device performance was contact-limited. R_CW was approximately 1×10^6 Ω cm at a V_G of −40 V. In contrast, the RW of the device composed of photopatterned PSS-wrapped MWNTs decreased consistently throughout the sweep of V_G from 0 to −40 V, indicating that RW was dominated by the channel resistance rather than R_CW; for this device, R_CW was less than 9×10^4 Ω cm at a V_G of −40 V.

Despite the 0.56 eV lower work function of the photopatterned PSS-wrapped MWNTs than that of gold, the contact resistance was much lower than that of OFET with gold, leading to higher mobility of transistor composed of photopatterned PSS-wrapped MWNTs. The lower contact resistance can originate from morphological change of TIPS-PEN and hole injection barrier between TIPS-PEN and electrode. The morphological changes of polycrystalline organic semiconductors such as vacuum-deposited pentacene and spin-coated soluble small-molecule semiconductor on different electrode surfaces were previously observed (40−43). However, in the case of drop-casted TIPS-PEN, we observed that large crystals were formed on the both the gold and the nanocomposite source/drain electrodes via channel and did not observe pronounced morphological difference of drop-casted TIPS-PEN on gold and photopatterned-MWNT using polarized optical microscopy (Figure 5a,b), consistent with the previously published result (44). Thus, we believe the lower contact resistance of OFET containing photopatterned PSS-wrapped MWNTs originated from hole injection barrier rather than morphological difference of TIPS-PEN on both electrodes. Many researchers report that the hole injection barrier between organic semiconductor and electrode was determined not only by the work function of electrodes, but also by whether the electrode surface was organic or metal (40, 43, 45). Despite the high work function of gold, the hole injection barrier at the interface between organic semiconductor and gold is large due to a large vacuum level shift. The large vacuum level shift is generally known to arise from the high induced density of interface states (IDIS) generated by the strong local orbital exchange and the potential correlation between the metal and the semiconductor (46). In contrast, the vacuum level shift between organic semiconductor and electrodes having an organic surface is small because of a low IDIS caused by the absence of the strong local orbital exchange and the potential correlation at the interface (40, 43). Therefore, the hole injection barrier between organic semiconductor and organic electrode is generally smaller than that between organic semiconductor and metal. This implies that the interface between TIPS-PEN and gold suffers from a large vacuum level shift, leading to a higher hole injection barrier. In contrast, the vacuum level shift between TIPS-PEN and photopatterned PSS-wrapped MWNTs is small and it results in a lower hole injection barrier leading to lower contact resistance (below 9×10^4 Ω cm) (47) of transistor based on photopatterned PSS-wrapped MWNTs than that of the transistors composed of gold source/drain electrodes (1×10^6 Ω cm).

CONCLUSIONS

PSS was observed to cross-link via UV exposure under a vacuum, indicating that PSS-wrapped MWNTs are photopatternable. FT-IR and XPS results suggested that the photo-crosslinking of PSS proceeded via a radical-coupling reaction initiated by UV cleavage of hydrogen atoms in the chain. During photo-crosslinking, cleavage of a significant fraction of the sulfonic acid groups occurred, which reduced the work function of PSS-wrapped MWNTs from 4.83 to 4.53 eV. The mobility of the TIPS-PEN field-effect transistors fabricated using PSS-wrapped MWNTs as source/drain electrodes was measured to be 0.134 ± 0.056 cm^2/(V s) with an on/off ratio of 1.5×10^5, about 12 times higher than that of transistors fabricated using gold source/drain electrodes (0.011 ± 0.004 cm^2/(V s)). The good performance of TIPS-PEN transistors with photopatterned PSS-wrapped MWNTs suggests that the photopatterned PSS-wrapped MWNTs are suitable for use as source/drain electrode materials for OFETs.

Acknowledgment. This work was supported by a grant from the Korea Science and Engineering Foundation (KOSEF) grant funded by the Korea government (MEST) (Grant 2010-0000809). The authors thank the Pohang Accelerator Laboratory for providing the 4B1 beamline (PES II) used in this study.

REFERENCES AND NOTES

(1) Dimitrakopoulos, C. D.; Malenfant, P. R. L. *Adv. Mater.* **2002**, *14*, 99.
(2) B.Crone, B.;A.; Dodabalapur, A.; Lin, Y.-Y.; Filas, R. W.; Bao, Z.; Laduca, A.; Sarpeshkar, R.; Katz, H. E.; Li, W. *Nature* **2000**, *403*, 521.
(3) Sirringhaus, H.; Tessler, N.; Friend, R. H. *Science* **1998**, *280*, 1741.
(4) Anthony, J. E.; Brooks, J. S.; Eaton, D. L.; arkin, S. R. *J. Am. Chem. Soc.* **2001**, *123*, 9482.
(5) Horowitz, G.; Hajlaoui, M. E.; Hajlaoui, R. *J. Appl. Phys.* **2000**, *87*, 4456.
(6) Mcculloch, I.; Heeney, M.; Bailey, C.; Genevicius, K.; Macdonald, I.; Shkunov, M.; Sparrowe, D.; Tierney, S.; Wagner, R.; Zhang, W.; Chabinyc, M. L.; Kline, R. J.; Mcgehee, M. D.; Toney, M. F. *Nat. Mater.* **2006**, *5*, 328.
(7) Hatton, R. A.; Miller, A. J.; Silva, S. R. P. *J. Mater. Chem.* **2008**, *18*, 1183.
(8) Ajayan, P. M.; Ebbsen, T. W. *Rep. Prog. Phys.* **1997**, *60*, 1025.
(9) Liu, J.; Rinzler, A. G.; Dai, H. J.; Hafner, H. J.; Bradley, R. K.; Boul, P. J.; Lu, A.; Iverson, T.; Shelimov, K.; Huffman, C. B.; Rodriguez-Marcias, F. J.; Shon, Y. S.; Lee, T. R.; Cobert, D. T.; Smalley, R. E. *Science* **1998**, *280*, 1253.
(10) Tenent, R. C.; Barnes, T. M.; Bergeson, J. D.; Ferguson, A. J.; To, B.; Gedvilas, L. M.; Heben, M. J.; Blackburn, J. L. *Adv. Mater.* **2009**, *21*, 3210.

(11) De, S.; Lyons, P. E.; Sorel, S.; Doherty, E. M.; King, P. J.; Blau, W. J.; Nirmalraj, P. N.; Boland, J. J.; Scardaci, V.; Joimel, J.; Coleman, J. N. *ACS Nano* **2009**, *3*, 714.
(12) O'connel, M. J.; Boul, P.; Ericson, L. M.; Huffman, C.; Wang, Y.; Haroz, E.; Kuper, C.; Tour, J.; Ausman, K. D.; Smalley, R. E. *Chem. Phys. Lett.* **2001**, *342*, 265.
(13) Liu, A.; Honma, I.; Ichihara, M.; Zhou, H. *Nanotechnology* **2006**, *17*, 2845.
(14) Kim, J.-B.; Premukumar, T.; Lee, K.; Geckeler, K. E. *Macromol. Rapid Commun.* **2007**, *28*, 276.
(15) Hong, K.; Nam, S.; Yang, C.; Kim, S. H.; Chung, D. S.; Yun, W. M.; Park, C. E. *Org. Electron.* **2009**, *10*, 363.
(16) Hong, K.; Yang, C.; Kim, S. H.; Jang, J.; Nam, S.; Park, C. E. *ACS Appl. Mater. Interface* **2009**, *1*, 2332.
(17) Zhang, Y. Y.; Shi, Y.; Chen, F.; Mhaisalkar, S. G.; Li, L.-J.; Ong, B. S. *Appl. Phys. Lett.* **2007**, *91*, 223512.
(18) Williams, C. D.; Robles, R. O.; Zhang, M.; Li, S.; Baughman, R. H.; Zakhidov, A. A. *Appl. Phys. Lett.* **2008**, *93*, 183506.
(19) Aguirre, C. M.; Auvray, S. S.; Pigeon, S.; Izquierdo, R.; Desjardins, P.; Martel, R. *Appl. Phys. Lett.* **2006**, *88*, 183104.
(20) Rowell, M. W.; Topinka1, M. A.; McGehee, M. D.; Prall, H.-J.; Dennler, G.; Sariciftci, N. S.; Hu, L.; Gruner, G. *Appl. Phys. Lett.* **2006**, *88*, 233506.
(21) Lee, K. S.; Banchet, G. B.; Gao, F.; Loo, Y.-L. *Appl. Phys. Lett.* **2005**, *86*, 074102.
(22) Sirringhaus, H.; Kawase, T.; Friend, R. H.; Shimoda, T.; Inbasekaran, M.; Wu, W.; Woo, E. P. *Science* **2000**, *290*, 2123.
(23) Kumar, A.; Whiteside, G. M. *Appl. Phys. Lett.* **1993**, *63*, 2002.
(24) Chou, S. Y.; Krauss, P. R.; Renstorm, P. J. *Appl. Phys. Lett.* **1996**, *67*, 3114.
(25) Bao, Z.; Feng, Y.; Dodabalapur, A.; Raju, V. R.; Lovinger, A. J. *Chem. Matter.* **1997**, *9*, 1299.
(26) Jang, Y.; Park, Y. D.; Lim, J. A.; Lee, H. S.; Lee, W. H.; Cho, K. *Appl. Phys. Lett.* **2006**, *89*, 183501.
(27) Menard, E.; Meitl, M. A.; Sun, Y.; Park, J.-U.; Shir, D. J.-L.; Nam, Y.-S.; Jeon, S.; Rogers, J. A. *Chem. Rev.* **2007**, *107*, 1117.
(28) Khong, S. H.; Sivaramakrishnan, S.; Png, R.-Q.; Wong, L.-Y.; Zhou, M.; Chua, L.-L.; Ho, P. K. H. *Adv. Funct. Mater.* **2007**, *17*, 2490.
(29) Winroth, G.; Latini, G.; Credgington, D.; Wong, L.-Y.; Chua, L.-L.; Ho, P. K. H.; Cacialli, F. *Appl. Phys. Lett.* **2008**, *92*, 103308.
(30) Touwslager, F. J.; Willard, N. P.; Leeuw, D. M. *Appl. Phys. Lett.* **2002**, *81*, 4556.
(31) Jakubowska, M.; Achmatowicz, S.; Baltrušaitis, V.; Młoøniak, A.; Wyøkiewicz, I.; Zwierkowska, E. *Microelectron. Reliab.* **2008**, *48*, 860.
(32) Cheremisinoff, N. P. *Handbook of Polymer Science and Technology: Vol. 1 Synthesis and Properties*; Marcel Dekker: New York, 1989.
(33) The S2p1/2 peak at a binding energy of 163.2 eV appeared as the UV exposure time increased, and the binding energy corresponded to that of deoxidized sulfur moieties, such as sulfide or thiophene groups. The mechanism for their production from sulfonic acid was not apparent from the experimental FT-IR and XPS measurements.
(34) Socrates, G. *Infrared Characteristic Group Frequencies: Tables and Charts*, 2nd ed; John Wiley & Sons: New York, 1994.
(35) Weir, N. A.; Milkie, T. H. *J. Polym. Sci., Polym. Chem. Ed.* **1979**, *17*, 3735.
(36) Cahen, D.; Kahn, A. *Adv. Mater.* **2003**, *15*, 271.
(37) Sze, S. *Semiconductor Devices:Physics and Technology*, 2nd ed.; Wiley: New York, 1981.
(38) Kim, J.; Jeong, J.; Cho, H. D.; Lee, C.; Kim, S. O.; Kwon, S.-K.; Hong, Y. *J. Phys. D: Appl. Phys.* **2009**, *42*, 115107.
(39) Gupta, D.; Jeon, N.; Yoo, S. *Org. Electron.* **2008**, *9*, 1026.
(40) Hong, K.; Lee, J. W.; Yang, S. Y.; Shin, K.; Jeon, H.; Kim, S. H.; Yang, C.; Park, C. E. *Org. Electron.* **2008**, *9*, 21.
(41) Kymissis, I.; Dimitrakopoulos, C. D.; Purushothaman, S. *IEEE. Trans. Electron. Dev.* **2001**, *48*, 1060.
(42) Gundlach, D. J.; Royer, J. E.; Park, S. K.; Subramanian, S.; Jurchescu, O. D.; Hamadani, B. H.; Moad, A. J.; Kline, R. J.; Teague, L. C.; Kirillov, O.; Richter, C. A.; Kushmerick, J. G.; Richter, L. J.; Parkin, S. R.; Jackson, T. N.; Anthony, J. E. *Nat. Mater.* **2008**, *9*, 216.
(43) Hong, K.; Yang, S. Y.; Yang, C.; Kim, S. H.; Choi, D.; Park, C. E. *Org. Electron.* **2008**, *9*, 864.
(44) Hong, J.-P.; Park, A.-Y.; Lee, S.; Kang, J.; Shin, N.; Yoon, D. Y. *Appl. Phys. Lett.* **2008**, *92*, 143311.
(45) Wan, A.; Hwang, J.; Amy, F.; Kahn, A. *Org. Electron.* **2005**, *6*, 47.
(46) Vazquez, H.; Oszwaldowski, R.; Pou, P.; Ortega, J.; Perez, R.; Flores, F.; Kahn, A. *Europhys. Lett.* **2004**, *65*, 802.
(47) Chwang, A. B.; Frisbie, C. D. *J. Phys. Chem. B* **2000**, *104*, 12202.

AM1008826